ANALYSIS OF THE EFFECT OF DOPANT CONCENTRATION ON ZnS CRYSTAL STRUCTURE BASED ON THE SHAPE OF THE STACKING FAULTS ENERGY VS HEXAGONALITY FUNCTION

BY E. MICHALSKI, M. DEMIANIUK, S. KACZMAREK AND J. ŻMIJA

Institute of Technical Physics, Military Academy of Technology, Warsaw*

Results from the investigation of crystals with a polytypic structure and crystals with stacking faults resulting from Mn-doping of ZnS crystals during the growth are presented. The crystal structures for the entire range of changes of the stacking of layers, that is, from the parent structure of 3C through 6H and 4H polytypes and disordered structures, to the structure of 2H were examined. A theoretical analysis was made of the stacking faults energy (SFE) vs function of the hexagonality in the entire range of changes of the energy, from those with SFE equal to zero (3C), up to the maximum (2H). A qualitative agreement was found between the experimentally observed shape of structures vs concentration of dopants and the results expected theoretically based on considerations of SFE. On this basis, a new interpretation is presented for the dependence of the hexagonality of structures on the concentration of dopants.

1. Introduction

Lundquist (1948) and Hayashi (1960) stated that for crystals of SiC a correlation *exists* between the content of dopants of Al and the occurrence of polytype structures of 6H, 15R and 4H. Moreover, Ananyeva et al. (1967) and Antrashenko (1972) found that for crystals of ZnS the dopant of Al increases the hexagonality of a structure up to the stabilization of the 2H polytype.

A comprehensive study of the effects of some dopants on the ZnS structure was made by Kozielski (1976). An experimental relationship between the degree of structure hexagonality and the concentration of Al and Cd dopants was obtained. He interpreted the results introducing into the statistical theory the linear for Cd and square for Al relationships of the potential difference of hexagonal and regular layers on the concentration of the dopant. Moreover, he showed that the structures observed cannot result only from the statistical distribution of layers within a specific degree of hexagonality.

* Address: Wojskowa Akademia Techniczna, 01489 Warszawa 49, Poland.

Recently, the evaluation of stacking faults energy (SFE) of the polytype structure is considered to be a major factor in the investigation of the phenomenon of polytypism.

Tiwari, Rai and Srivastava (1974) were the first to use the method of Hirth—Lothe (1968) for computing the energy of single stacking faults by means of the model of elastic spheres coupled by central forces in considering the polytype structures in CdJ$_2$ crystals having a parent non-faulted 4H structure. SFE's have been calculated (Tiwari et a!. (1975), (1976) and Pandey, Krishna (1975)) to explain the occurrence of polytype series in crystals with initial 4H and 6H structures as well as to account for some specific transitions, e.g. 84R$_1$, 84R$_2$ due to temperature effects. It has been suggested to use the values of SFE as a criterion for the determination of polytype layer sequences in cases difficult to solve by X-ray analysis.

In this paper Mn-doped ZnS crystal structures have been investigated for dopant concentrations varying from 0.1 to 6.25% mole. The results are discussed by analysing the shape of the SFE vs. hexagonality function.

2. Experimental results

Manganium-doped zinc sulphide crystals used for the tests were grown from the melt phase under a pressurized argon atmosphere (Demianiuk, Żmija (1975)). The structures were examined by rotary and oscillating crystal methods using DKK-60 cameras and a RGNS-2 Weissenberg goniometer (2r = 5.72 cm). Samples were prepared by chipping-off small crystals (0.3 mm thick and 3 mm long), approximately oriented along the c-axis.

The manganium concentration was determined by chemical methods (Wieteska (1978)). The variations of dopant concentration in the volume zones analyzed (ca. 0.2 cm^3) sampled for structural tests were taken into account. The reproducibility of structures for the same Mn contents as found from preliminary investigations on many different crystals was sufficiently good.

The 10.l rows of X-ray diffraction photograph spots of test sets in order of increasing manganium concentration are shown in Fig. 1. In general, the concentration of hexagonal layers increases with the concentration of the dopant. According to Michalski et al. (1978) twin stacking faults in the 3C structures arise at low manganium concentrations. For higher manganium concentrations a layer arrangement typical for the 6H(33) polytype tends to dominate, with decreasing amounts of stacking faults in this new structure. At a manganium concentration of approx. 1.7 % mole the X-ray diffraction photographs show an almost pure 6H(33) structure. With still higher manganium concentrations the concentration of stacking faults tends to increase again, and finally, at ca. 2.5 % mole Mn, the 6H(33) structure changes entirely into 4H(22). Above 3.2% mole Mn the crystals have a pure 2H structure and no effect of a further increase in manganium concentration on the arrangement of the layers was observed.

It can be concluded, that the concentrations of Mn selected for the investigation covers the entire range of faulted and polytype structures. It is also clear that the manganium is a favourable element for testing the effect of dopants because it leads to the forma-
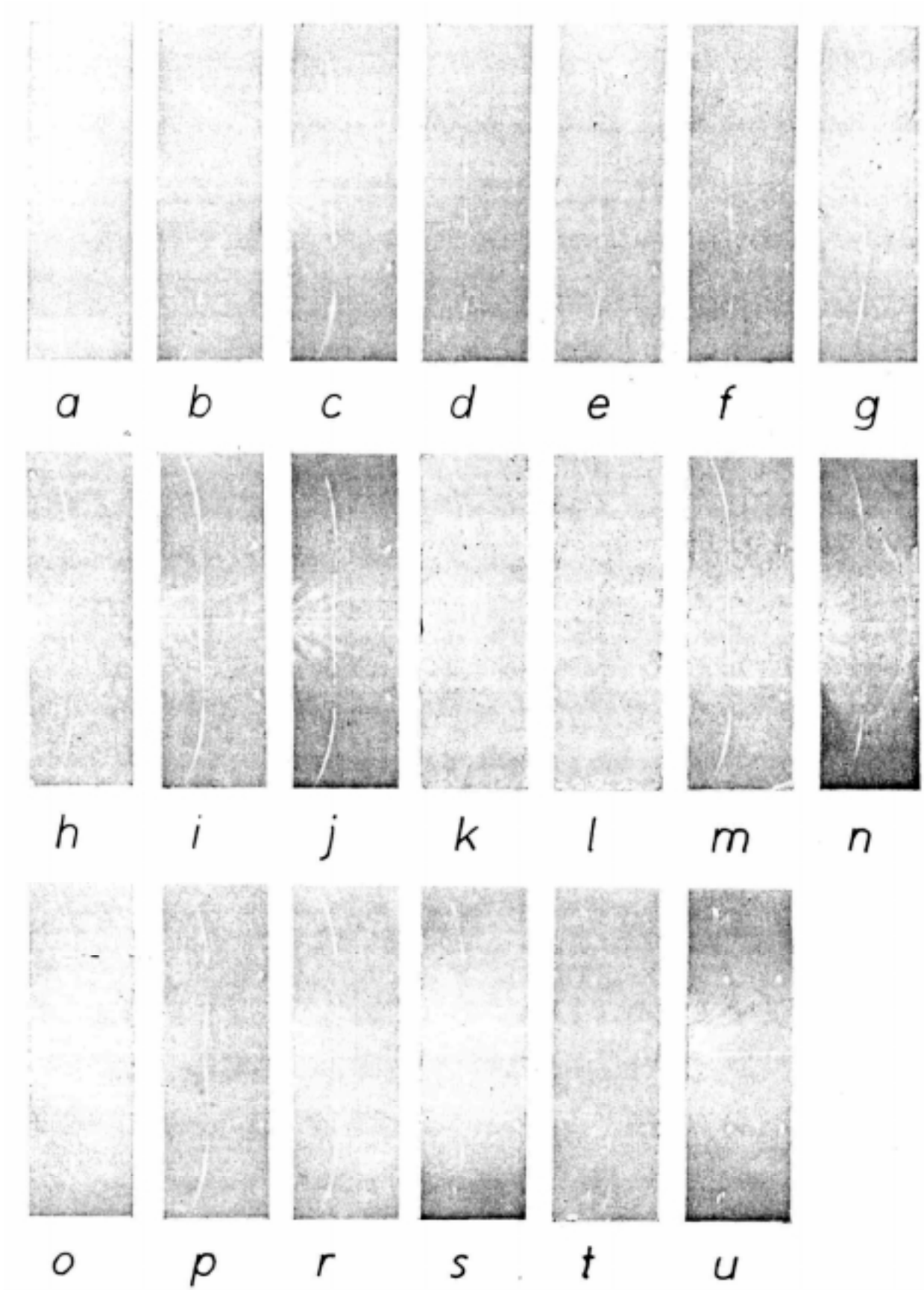
Fig. 1. The 10.*l* row of spots recorded on *c*-axis rotation photographs ($\lambda = 1.54$ Å 25 = 5.72 cm) of ZnS crystals with Mn concentrations (in % mole): a) 0.10, b) 0.65, c) 0.74, d) 0.83, e) 1.10, f) 1.21, g) 1.22, h) 1.26, i) 1.70, j) 1.76, k) 1.78, 1) 1.88, m) 2.16, n) 2.17, o) 2.36, p) 2.39, r) 2.50, s.) 2.59, t) 3.23, u) 6.25

tion of monocrystals having a degree of perfection sufficiently high for structural analysis. Moreover, the initial analysis of the X-ray diffraction photographs shows a specific shape of the structure hexagonality vs dopant concentration curve. An interesting physical significance can be attributed to this shape.

To plot the curve, a quantitative evaluation of the degree of structure hexagonality was performed based on the study of the X-ray diffraction photographs. The method of "model analysis" (Pałosz (1977)) was used. The theoretical intensity distribution along the $10.l$ row of spots for the assumed models of approximately 200 layers each was computed by the expression:

$$\sum_{-K(\Delta y)/2}^{+K(\Delta y)/2} \frac{I_{10.l+K(\Delta y)} \cdot (1-K^2(\Delta y) \cdot 10^{-3})}{[I_{10.l+K(\Delta y)} \cdot (1-K^2(\Delta y) \cdot 10^{-3})]_{\max}} = f(y_l), \tag{1}$$

where y_l is the coordinate of $10./$reflexes measured from the zero horizontal contour (mm) and according to Mirkin (1977) is related to Bragg's angle

$$y_l = 28.65 \cdot \text{tg arc cos} \frac{\cos 2\theta_l}{\cos 2\theta_{l=0}} . \tag{2}$$

$K(\Delta y)$ is the number of reflexes counted along the $10.l$ contour comprised within the Δy aperture reflex broadening (Δy is assumed to be a mean value of the measured broadening of 11.0 and $11.m$ reflex; here $\Delta y = 0.6$ mm). $I_{10.l}$ is the theoretical intensity of discrete reflex for ~ 200 layer models   I

$$I_{10.l} = (f_{Zn}'^2 + f_S^2 + f_{Zn}' f_S \cos 2\pi l p)(A_{Zn}^2 + B_{Zn}^2) \frac{1+\cos^2 2\theta_l}{\sin 2\theta_l} , \tag{3}$$

$$A_{Zn} = \sum_{n=0}^{n=m} \cos 2\pi(hx+ky+lz), \quad B_{Zn} = \sum_{n=0}^{n=m} \sin 2\pi(hx+ky+lz), \quad p = 3/4m, \tag{4}$$

where n is the number of consecutive layer in the structural model, m is the total quantity of layers in the model and x, y, z are values depending on the position of the layers:

	x	y	z
A	0	0	(n-1)/m
B	2/3	1/3	(n-1)/m
C	1/3	2/3	(n-1)/m

(5)

Bragg's angle results from

$$\sin \theta_{10.l} = \frac{\lambda}{2}\sqrt{a^{*2}+l^2 c^{*2}} = \frac{\lambda}{2}\sqrt{\left(\frac{2\sqrt{3}}{3a}\right)^2 + l^2\left(\frac{1}{mc}\right)^2}, \tag{6}$$

where $l = 0, ..., m;$ $a,$ c are parameters of the unit cell; λ — X-ray wavelength, f_{Zn} — modified factors of $Zn_{1-x}Mn_xS,$ $f'_{Zn} == (1-x)f_{Zn}+xf_{Mn}.$

The calculations have been made for 6H+DS polytype structure models with a varying "fault-order degree" α_b (defined as in Jagodzinski (1960)) for hexagonalities higher and lower than $\alpha_h = 1/3$ as well as for 3C+DS structures.

Curves obtained for 6H+DS structures exhibit in addition to the broadening resulting from the faulting, a characteristic change of intensity distribution in those positions which correspond to the reflexions, and the magnitude of this change depends on the degree of hexagonality. Viz., at higher hexagonality, the increase of "fault-order degree" is accompanied by an attenuation (with respect to the maximum intensity at 10.2) of 10.1, 10.3 and 10.5 reflex; while 10.4 reflexes are enhanced (Figs 2b, c). At lower hexagonalities 10.1, 10.4 and 10.5 reflexes are attenuated, while 10.3 is enhanced (Figs 2d, e).

Curves obtained for 3C+DS structures have more or less broadened maxima (or
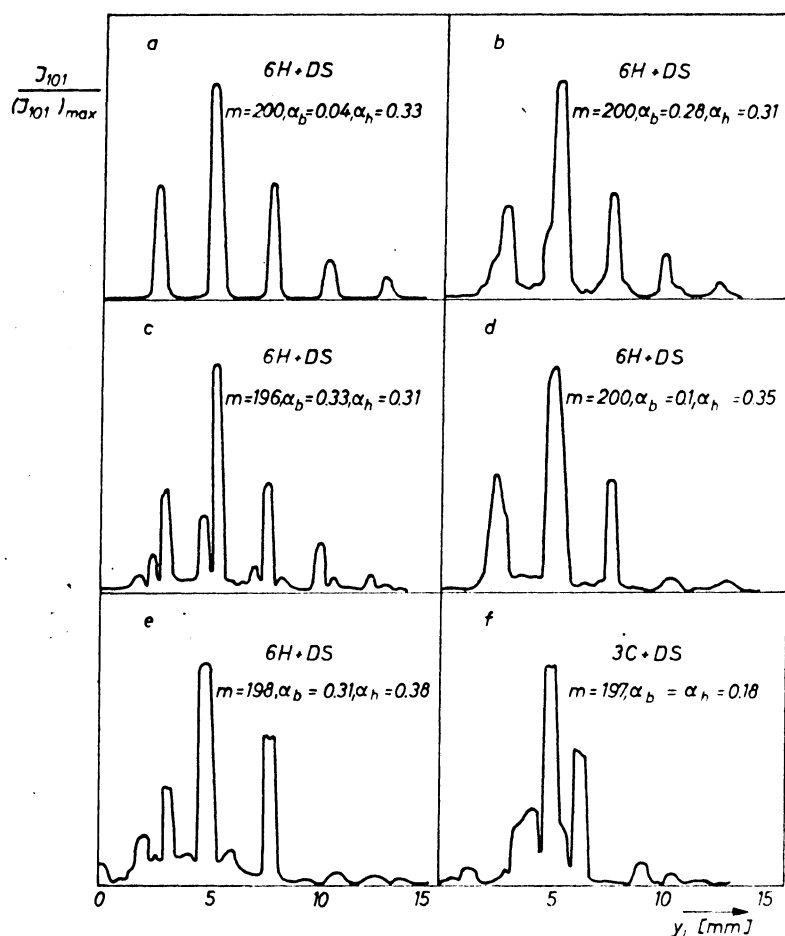

Fig. 2. Examples of theoretical curves of intensity distribution along the 10.l row from models with the following characteristics: α_b = fault-order degree, α_h = hexagonality, n = number of layers in the identity period
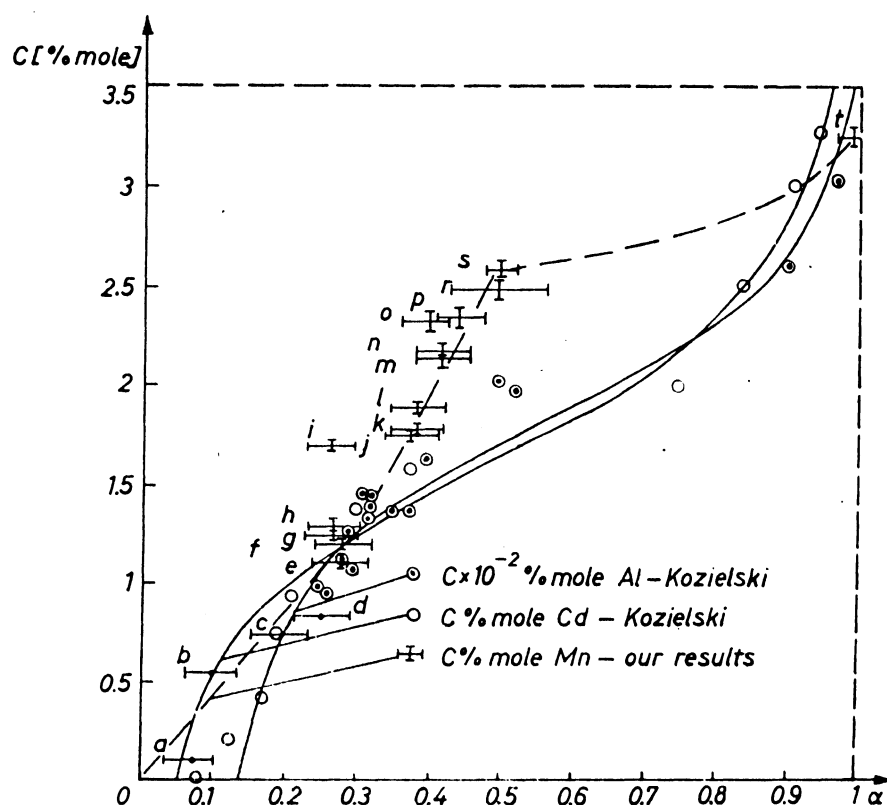
Fig. 3. Experimental dependence of structure hexagonality on dopant concentrations

groups of maxima) around the positions of 10.1 and 10.2 reflexes (3C structure) or 10.2 and 10.4 reflexes (structure 6H) as shown in Fig. 2f.

By comparing the photometring curves to those obtained theoretically, the degrees of hexagonality for the structures with stacking faults was determined with an accuracy of ± 5 % and with higher accuracy for the structure completely or almost completely free of faults.

The results have been plotted in c—α coordinates (Fig. 3) together with experimental points from the work by Kozielski (1976). The good agreement between our findings and Kozielski's results is seen. The greatest discrepancies are for very low manganium concentrations. In Kozielski's work, the plot starts for values corresponding to higher hexagonalities. This probably results either from different techniques of crystal growth of from the lower purity of Kozielski's crystals.

Since there is no reason to consider the lattice distortion energy to be related to the dopant concentration in a way similar to those reflected by the shape of the experimental curve, it can be assumed that this shape is determined by the SFE vs hexagonality function.

3. Analysis of the SFE vs hexagonality

In computing SFE for our ZnS crystals the Hirth-Lothe (1968) method was used for calculating the energy of individual stacking faults. This method is based on the model of elastic spheres coupled by central forces, as was used by Tiwari et al. (1974, 1975) and Pandey and Krishna (1975), for CdJ_2 and SiC crystals.

According to this model, the SFE can be represented by the sum of products of the quantity of faulted pairs of layers spaced by n - layers and the respective distortion energy of these pairs, Ψ_n. The energy of faulted pairs spaced by more than 4 layers can be neglected. As will be shown below, this assumption greatly simplifies the computation introducing only a minor reduction in the accuracy.

The quantity of faulted pairs of layers spaced by n – layers is determined by summing all those pairs which have mutual positions other than those "correct" for the parent non-faulted structure.

In practice, for structures containing double ion layers (e.g., ZnS), the positions of one type of ions determines the correct or incorrect mutual positions of pairs because the positions of other types of ions are determined already.

Therefore, to represent the elastic spheres in the model, ion pairs, e.g., ZnS, not displaced in the stacking fault zones are taken into account rather than the individual ions of each type.

Since the 3C structure is known to be characteristic for the parent non-faulted structure of ZnS crystals grown from the melt of high purity input materials, all pairs spaced by 3 layers in identical positions and those spaced by 2 and 4 layers in different positions are considered as being faulted (Fig. 4).

The distortion energy of the individual pair of layers is calculated as an absolute value of the difference between the sum of bond energies of the individual spheres of a pair of layers in the faulted structures and in the normal 3C structure.

```
                                    B . A      B . . B     C . . . A
            3C
                                    C . B      C . . C     A . . . B

       a)  ABCABCABCABC            A . C      A . . A     B . . . C


       b)  ABCABACBACB            A . A      C . . A     C . . . C
```
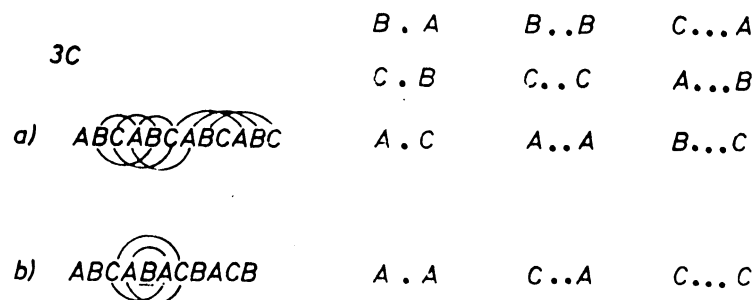
Fig. 4. a) Normal positions of layer pairs spaced by 2,3 and 4 layers in the 3C structure, b) Faulted positions, due to layer arrangement faults spaced by 2,3 and 4 layers

The bond lengths and the layer pair distortion energies expressed in the terms of the technique presented by Tiwari et al. (1974) were calculated by considering the projection of all spheres from the layers above the one selected projection plane on this plane and on a perpendicular plane (Fig. 5). The lengths of r_n^j vectors which link a sphere of the selected layer to the spheres of another layer (spaced by n – layers) was determined by taking into account the height, h_n, of the layer which contains these atoms, as well as the values of vector projections, r^j, on the selected layer plane

$$r_n^j = ((r^j)^2 + (h_n)^2)^{1/2}, \qquad (7)$$

where n is the index indicating the layer which contains the given sphere by specifying the distance of the selected layer expressed in the quantity of layer spacings, j is the index

indicating the radius of the circle which contains the given sphere in the projection on the selected layer plane by specifying the consecutive number of the radius in a sequence from the smallest one to the largest.

According to Fig. 5 the consecutive values of r^j for $j = 0, 1, 2, ...$ amount to $0, 2/3(\sqrt{3}/2)a$, $a, 4/3(\sqrt{3}/2)a, \sqrt{((a+a/2)^2 + (a\sqrt{3}/6)^2)}, ...$ respectively, with a denoting the distance between the spheres in the layer.

The consecutive values of h_n amount to $n\sqrt{2}/3a$, with $n = 1, 2, ...$ Now, expression (7) can be used to determine the r_n^j for all possible sphere positions.
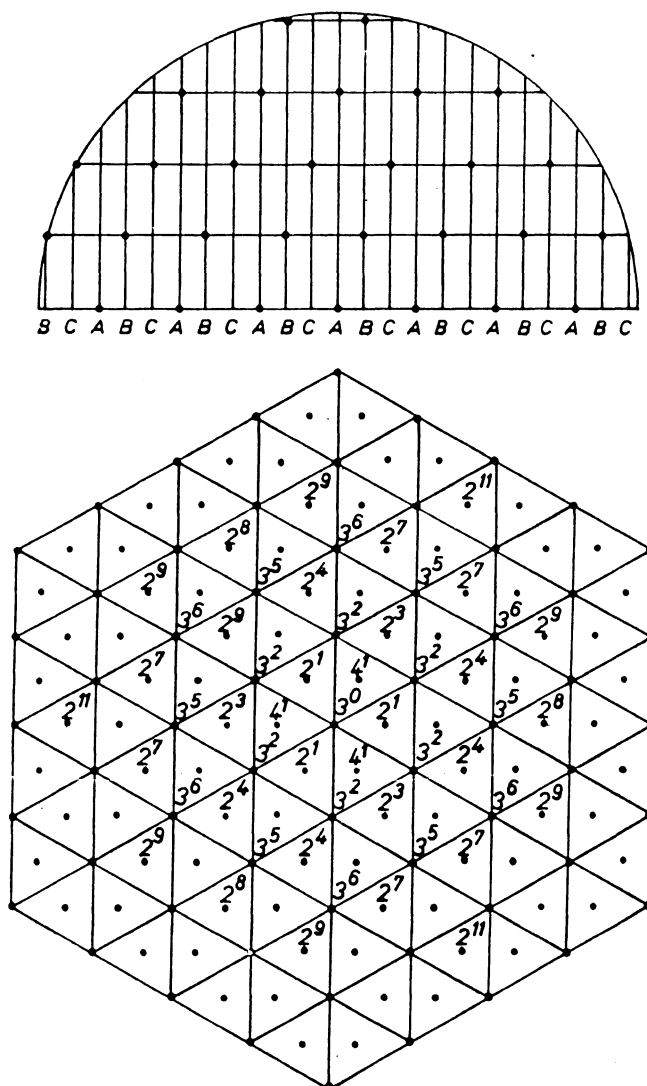

Fig. 5. Projection of the spheres of the 3C structure model on the plane of a selected layer and on a plane perpendicular to the latter. In the designation of m^j spheres (at the end of r_n^j vectors which link them to the sphere of the selected layer), n indicates the layer of the given sphere, j indicates the radius of the circle containing the given atom in its projection on the selected layer plane

It can be seen from Fig. 5 that for layer positions characteristic for the 3C structure, the following r_n^j vectors, linking the spheres of the n - spaced layers, $r^1_2, r^3_2, r^4_2, r^7_2, r^8_2, r^{11}_2, r^0_3, r^2_3, r^5_3, r^6_3, r^1_4,$ occur among all the ones generally possible.

The remaining vectors will appear only for faulted positions of layers. Therefore, these vectors are in paranthesis in Table I e.g., $r^0_2{}'$, $r^2_2{}'$ etc.

The distortion energy of the individual pair of layers, Ψ_n is now represented by the difference in the energy of the bond, $\phi_n^j{}'$, (spheres at a distance of $r_n^j{}'$) and the bond energy, ϕ_n^j (spheres at a distance of r_n^j) and taking into account the quantity of those bonds.

The values of the radius as well as a sequence of bond energies for the individual layers spaced by 2, 3 and 4 layers, positioned at normal and faulted positions with respect to the 3C structure are shown in Table I.

According to Table I the distortion energies of the individual pair of layers are expressed by the bond energies as follows:

$$\Psi_2 = |(\varphi_2^{0'} + 6\varphi_2^{2'} + 6\varphi_2^{5'} + 6\varphi_2^{6'} + 12\varphi_2^{10'}) + (3\varphi_2^1 + 3\varphi_2^3 + 6\varphi_2^4 + 6\varphi_2^7 + 3\varphi_2^8 + 6\varphi_2^9 + 3\varphi_2^{11})|,$$

$$\Psi_3 = |(3\varphi_3^{1'} + 3\varphi_3^{3'} + 6\varphi_3^{4'} + 6\varphi_3^{7'}) - (\varphi_3^0 + 6\varphi_3^2 + 6\varphi_3^5 + 6\varphi_3^6)|,$$

$$\Psi_4 = |\varphi_4^{0'} - 3\varphi_4^1| . \tag{8}$$

TABLE I

Expressing Ψ_n in terms of ϕ_n^j

Height of layer	$r_{A.C}^B$ magnitude of r_n^j (in units of a)	Bond energy φ_n^j	No. of bonds having same length	$r_{A.A}$ magnitude of r_n^j (in units of a)	Bond energy $\varphi_n^{j'}$	No. of bonds having same length
$2\sqrt{\frac{2}{3}}\,a$	$r_2^1 = \sqrt{3}$	φ_2^1	3	$r_2^{0'} = \sqrt{\frac{8}{3}}$	$\varphi_2^{0'}$	1
	$r_2^3 = \sqrt{4}$	φ_2^3	3	$r_2^{2'} = \sqrt{\frac{11}{3}}$	$\varphi_3^{2'}$	6
	$r_2^4 = \sqrt{5}$	φ_2^4	6	$r_2^{5'} = \sqrt{\frac{17}{3}}$	φ_2^5	6
	$r_2^7 = \sqrt{7}$	φ_2^7	6	$r_2^{6'} = \sqrt{\frac{20}{3}}$	$\varphi_2^{6'}$	6
	$r_2^8 = \sqrt{8}$	φ_2^8	3	$r_2^{10'} = \sqrt{\frac{29}{3}}$	$\varphi_2^{10'}$	12
	$r_2^9 = \sqrt{9}$	φ_2^9	6			
	$r_2^{11} = \sqrt{11}$	φ_2^{11}	3			
	$r_{A..A}$			$r_{A..C}^B$		
$3\sqrt{\frac{2}{3}}\,a$	$r_3^0 = \sqrt{6}$	φ_3^0	1	$r_3^{1'} = \sqrt{\frac{19}{3}}$	$\varphi_3^{1'}$	3
	$r_3^2 = \sqrt{7}$	φ_3^2	6	$r_3^{3'} = \sqrt{\frac{22}{3}}$	$\varphi_3^{3'}$	3
	$r_3^5 = \sqrt{9}$	φ_3^5	6	$r_3^{4'} = \sqrt{\frac{25}{3}}$	$\varphi_3^{4'}$	6
	$r_3^6 = \sqrt{10}$	φ_3^6	6	$r_3^{7'} = \sqrt{\frac{31}{3}}$	$\varphi_3^{7'}$	6
$4\sqrt{\frac{2}{3}}\,a$	$r_{A...C}^B$			$r_{A...A}$		
	$r_4^1 = \sqrt{11}$	φ_4^1	3	$r_4^{0'} = \sqrt{\frac{32}{3}}$	$\varphi_4^{0'}$	1

However, no quantitative calculations can proceed without introducing into the model an accurate knowledge of the influence of the distance between the spheres on the value of the bond energy. We were not able to determine the character of this dependence theoretically, because it describes the interaction between spheres which, as results from the model, represents pairs of ions of Zn-S which are not displaced in the stacking fault zone. To date this specific change of energy vs. length of bonds has not been described.
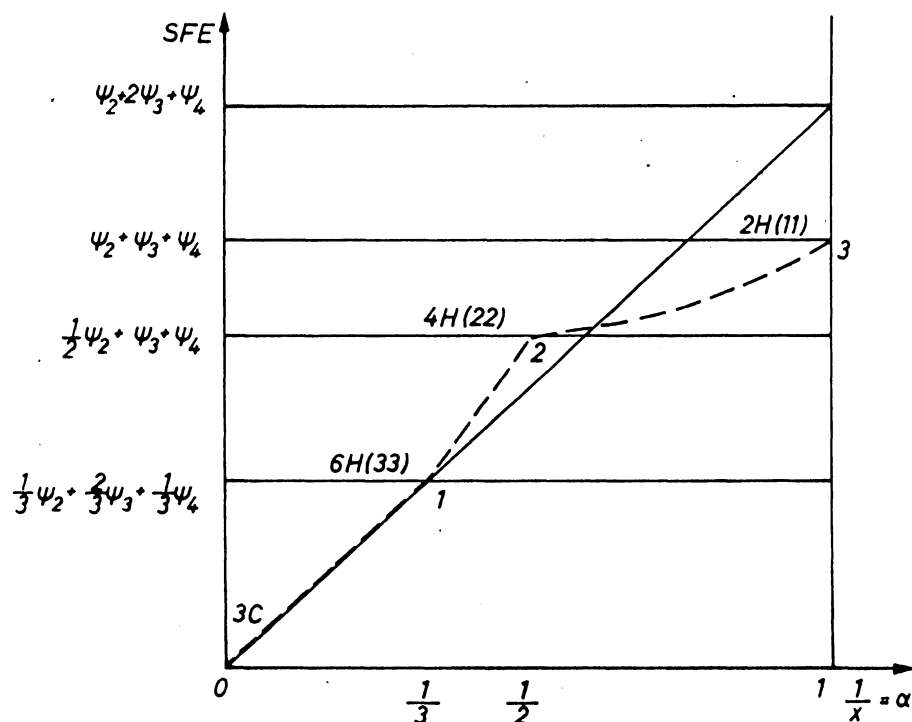

Fig. 6. Polytype- and faulted-arrangement structures; SFE-vs. $(\alpha = 1/x$, assuming $\Psi_2 = 3/2\Psi_3 = 2\Psi_4$. The 0-1-2-3 curve can be expressed as follows: section 0-1: SFE = $(2\Psi_2 + 4\Psi_3 + 2\Psi_4)/2x$, section 1-2: SFE = $(2\Psi_2 + 4\Psi_3 + 2\Psi_4)/2x + (1/x - 1/3)3\Psi_4$, section 2-3: SFE = $2\Psi_4/2x + \Psi_3 + y \cdot \Psi_4$ with y taking the value of unity at points 2 and 3, while varying from 0 to unity between them

Considering that ϕ decreases for the more distant spheres we can theoretically obtain only the following relation between Ψ_n values $\Psi_2 = K_1 \cdot \Psi_3 = K_2 \cdot \Psi_4$ where $K_2 > K_1 > 1$. To make more qualitatively considerations, we have assumed, that the changes in values of Ψ_2, Ψ_3, Ψ_4 are inversely proportional to the distance of layers $\Psi_2 = 2/3\Psi_3 = 2\Psi_4$. This assumption, as shown below, does not limit the generality of our conclusions. By using this assumption all ordered and disordered polytype structures have been displayed on the plot in Fig. 6 in coordinates SFE and $\alpha = 1/x$, where α is the degree of hexagonality and x is average area of zones with a unique sequence of layers.

It is seen that the structures which contain in Zdanov's symbol numbers equal to the inverse of hexagonality $x = 1/\alpha$ (i.e., equal to the average area of zones with a unique sequence of layers) or to the nearest whole numbers if x is not an integer follow the 0-1-2-3 curve.

The structures which contain a "1" in Zdanov's symbol lie on the right of the 0-1 section of the curve, i.e., in the zone of increased hexagonality but the same SFE. Those containing a "2" are placed on the left of the 0-1 section of the curve, i.e., in the

zone of lower hexagonality and SFE's equal to those on the 0-1 section. Structures with equal energies containing a "1" and a "2" lie on the left or on the right, according to the part of these numbers on either of the zones.

The above results from the fact that the energy of a pair of adjacent hexagonal layers (Fig. 7a) which render an intrinsic stacking fault (a "1" in Zdanov's symbol) is lower than that at two spaced hexagonal layers (Fig. 7c) (at two twinning stacking faults). While the energy of a 2-layer-spaced hexagonal layer pair (Fig. 7b) renders an extrinsic stacking fault or a "2" in Zdanov's symbol, exceeds that of two separate hexagonal layers.

$$SFE = 2\Psi_2 + 3\Psi_3$$

$$SFE = 2\Psi_2 + 4\Psi_3 + 3\Psi_4$$

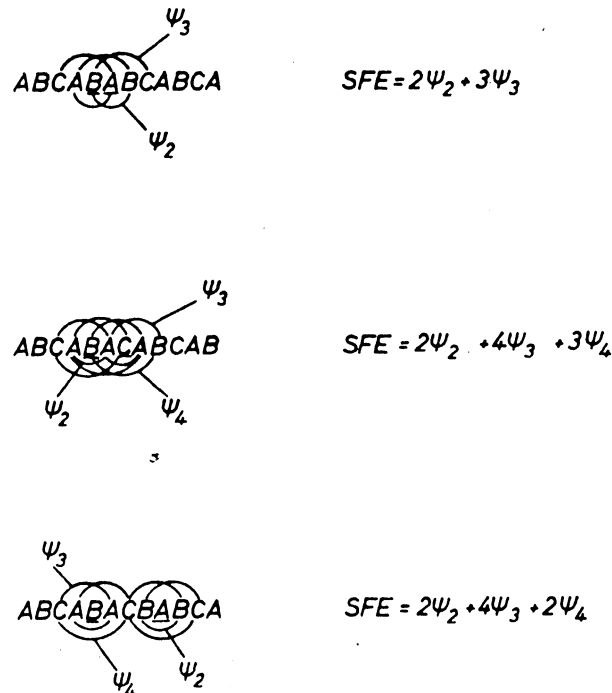
$$SFE = 2\Psi_2 + 4\Psi_3 + 2\Psi_4$$

Fig. 7. SFE's of structures with two hexagonal layers; a) adjacent one to the other, b) spaced by two layers, c) spaced by more than two layers

It can be concluded that for equal SFE's the number of "faulted" hexagonal layers in respect to the 3C structure is greater for adjacent hexagonal layers than for 2-layer-spaced layers.

A similar explanation can be given for the structures which are on the right and left of the 1-2-3 section of the, curve. .

It can be seen that the characteristic shape of the 0-1-2-3 curve (Fig. 6) is not influenced by the values of Ψ_2, Ψ_3 and Ψ_4. This means that the section 0-1, representing the sum of equal energies of the individual twinning stacking faults vs. the quantity of the faults is a straight line. Over the 1-2 section, the increased amount of faulted pairs of layers spaced by four layers and due to the occurence of extrinsic stacking faults (a "2" in Zdanov's symbol for these structures) requires additional SFE besides that needed to compensate for the increase of hexagonality from section 0-1

$$SFE = \frac{2\Psi_2 + 4\Psi_3 + 2\Psi_4}{2x} + \left(\frac{1}{x} - \frac{1}{3}\right)3\Psi_4. \tag{9}$$

The second term of this expression represents the increase of energy needed for the arrangement of an additional 4-layer-spaced pair of faulted layers. This effect gives rise to the bending at the top of the 1-2 section. A similar consideration leads to the explanation of the characteristic shape of the remaining, 2-3, portion of the curve.

4. Discussion

When comparing Figs 3 and 6 it can be seen that the shape of the experimental curves fits well to that of the 0-1-2-3 theoretical curve. Moreover, it can be noted, that an approximation which-neglects the distortion of pairs of layers spaced by more than .4 layers is justified for such an investigation because pure polytype structures, 6H, 4H and 2H, found in the plot do not reveal faulted pairs spaced by 5 layers. The positions of 5-layer-spaced pairs of layers in 3C, 6H, 4H and 2H structures is. shown in Fig. 8. This advantageous situation greatly reduces the error in determining the SFE of these ordered polytype
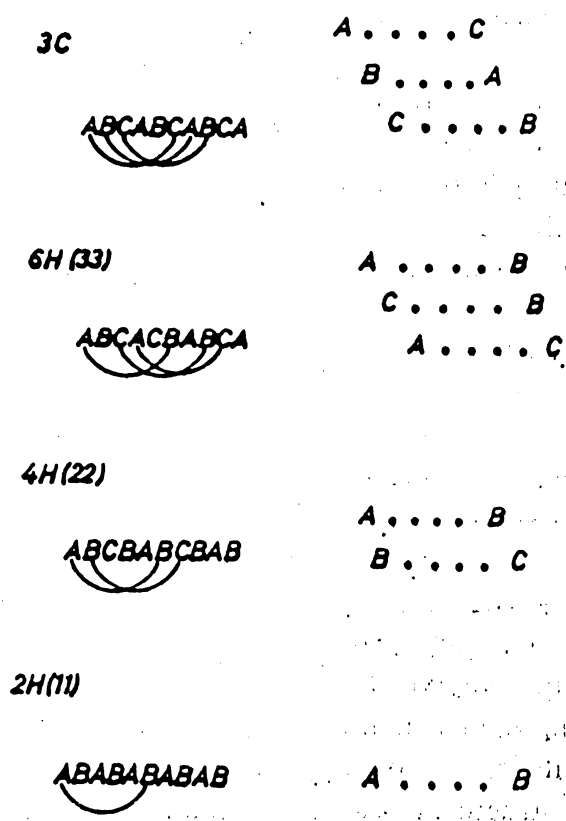

Fig. 8. Positions of layer pairs, spaced by 5 layers, in 3C, 6H, 4H, and 2H structures

structures due to the approximation neglecting the effect resulting from the position of spheres in the more distant coordination. However, a larger error can be encountered for disordered structures.

On the other hand, the positions of ordered polytype structures are determined more accurately than those incompletely ordered. Therefore, it is of special importance that we can observe a very good agreement of the characteristic positions of the ordered polytype structures of 6H, 4H, 2H on the experimental and theoretical curves.

Moreover, it can be noted, that except for cases of extremely low dopant concentrations, the experimental points of Kozielski (1976) for Al and Cd dopants are on the curves which are qualitatively in agreement with the theoretical SFE vs. hexagonality curve. This is within the range of error which does not exceed the one resulting from the curves obtained by Kozielski (1976) and expressed as

$$\alpha = 1/2\,(1 + \text{th}\ V(c)/kT). \tag{10}$$

The considerations discussed above can imply that the dependence of SFE vs. hexagonality can decide the character of the dependence between the hexagonality structures and the concentration of dopants.

It is appropriate to determine what is responsible for the selection of structures which fit the 0-1-2-3 curve among the wide variety of those which bear the same SFE. The classical model of spheres with central interaction forces unfortunately fails to answer the question.
It can be predicted, however, as was done by Schneer (1955), that the burden of responsibility is due to some unknown order-setting long-range quantum effects similar to those responsible for the long-range order-setting effects in ferromagnetics.

It can be noted that the structures which have Zdanov's symbol numbers equal or nearest to the mean magnitude of zones with a unique layer sequence feature the most uniform arrangement of the hexagonal layers and thus offer a maximum amount of contacts between the layers which are in various positions. This is in compliance with Schneer's theory of the potential of order-setting interactions, *Em(ij)* which is higher between the layers with equal positions than between the layers of different positions. However, the theory does not explain the nature of the order-setting forces nor the fact that no polytypes have been found with faulted structures of hexagonalities other than 0, 1/3, 1/2 and 1.

The vibration entropy from Jagodzinski's (1954) theory plays an important part in these mechanisms, but oscillation spectra for ZnS crystals with polytype structures and containing stacking faults have not been calculated yet. The problem seems to be of major importance for the theory of polytypism.

This paper extends the validity of the model of elastic spheres coupled by central forces not only for the single polytype transitions observed to date, but also to the wide range of polytypes and stacking-fault containing structures.

It seems evident that similar investigations would also be interesting for crystals with more ordered polytype structures because of changes in the stacking of layers arid for crystals with other parent structures.

REFERENCES

Ananyeva, G. V., Dubenskii, K. K.,Ryskin, A.L, Chiiko, G.L., *Solid State Phys.* **10**, 1800(1968).

Antrashenko, I. P., *Izv. Akad. Nauk Neorg. Mater.* **8,** 639 (1972).

Demianiuk, M., Żmija J., *Biul. WAT* **24**, 105 (1975).

Hayashi, A., *J. Mineral Soc. Japan* **4,** 363 (1960).

Hirth, J. P., Lothe J., *Theory of Dislocations,* Me Graw-Hill. Inc. 1968.

Jagodziński, H., *Acta Cryst.* **7**, 300 (1954).

Jagodziński, H., *Neues Jahrb. Miner. Monatsh.* **3**, 49 (1954).

Jagodziński, H., Arnold, H., *Silicon Carbide,* Proc. Conf. Boston 1959, Pergamon Press, New York 1960, p. 136.

Kozielski, M. J., Reports of the Institute of Physics, Warsaw Technical University 1976, p. 16.

Lundquist, D., *Acta Chem. Scand.* 2, 177 (1948).

Michalski, E., Demianiuk, M., Żmija J., *Electron Technology* **5**, (1978).

Mirkin, L. I., *Rentgenostrukturnyi analiz,* Izd. Nauka 1976.

Patosz, B., Dissertation work, Warsaw Technical University 1977.

Pandey, D. Krishna, P., *Phil. Mag.* **31,** 1113 (1973).

Pandey, D., Krishna P., *Phys. Lett.* **51A,** 209 (1975).

Pandey, D., Krishna, P., *J. Cryst. Growth* **31,** 66 (1975).

Rai, A. K., Tiwari, R. S., Srivastava, 0. N., *J. Cryst. Growth* **36,** 71 (1976).

Schneer, C. J., *Acta Cryst.* **8,** 279 (1955).

Tiwari, R. S., Rai, A. K., Srivastava, 0. N., *Phys. Rev.* **139,** 5155 (1974).

Tiwari, R. S., Rai, A. K., Srivastava, P. N., *Phys. Status Solidi* (a) **31,** 419 (1975).

Verma, A. R., Krishna, P., *Polymorphism and Polytypism in Crystals,* John Wiley & Sons Inc. 1966.

Wieteska, E., unpublished results, 1976